Optofluidic distributed feedback lasers with evanescent pumping: Reduced threshold and angular dispersion analysis

Markus Karl, Guy L. Whitworth, Marcel Schubert, Christof P. Dietrich, Ifor D. W. Samuel, Graham A. Turnbull, and Malte C. Gather

Articles you may be interested in

Photonic stopband tuning of organic semiconductor distributed feedback lasers by oblique angle deposition of an intermediate high index layer
Appl. Phys. Lett. **95**, 021112 (2009); 10.1063/1.3184591

Widely tunable distributed-feedback lasers with chirped gratings
Appl. Phys. Lett. **94**, 161102 (2009); 10.1063/1.3123813

Effect of gain localization in circular-grating distributed feedback lasers
Appl. Phys. Lett. **87**, 201101 (2005); 10.1063/1.2120915

1.55 μm single mode lasers with complex coupled distributed feedback gratings fabricated by focused ion beam implantation
Appl. Phys. Lett. **75**, 1491 (1999); 10.1063/1.124732

Low-threshold high-quantum-efficiency laterally gain-coupled InGaAs/AlGaAs distributed feedback lasers
Appl. Phys. Lett. **74**, 483 (1999); 10.1063/1.123164

AIP | Applied Physics Reviews

NEW Special Topic Sections

NOW ONLINE
Lithium Niobate Properties and Applications: Reviews of Emerging Trends

AIP | Applied Physics Reviews

Optofluidic distributed feedback lasers with evanescent pumping: Reduced threshold and angular dispersion analysis

Markus Karl, Guy L. Whitworth, Marcel Schubert, Christof P. Dietrich, Ifor D. W. Samuel, Graham A. Turnbull, and Malte C. Gather[a)]

Organic Semiconductor Centre, SUPA, School of Physics and Astronomy, University of St Andrews, St Andrews, Fife KY16 9SS, United Kingdom

We demonstrate an evanescently pumped water-based optofluidic distributed feedback (DFB) laser with a record low pump threshold of $E_{TH} = 520$ nJ. The low threshold results from an optimized mode shape, which is achieved by a low refractive index substrate, and from the use of a mixed-order DFB grating. Investigating the photonic band structure via angular dispersion analysis both above and below lasing threshold allows us to measure the refractive index of the liquid gain layer and to determine the device parameters such as the waveguide core layer thickness. We show that it is possible to tailor the divergence of the lasing emission by varying the number of second order grating periods used for outcoupling. © *2016 Author(s). All article content, except where otherwise noted, is licensed under a Creative Commons Attribution (CC BY) license (http://creativecommons.org/licenses/by/4.0/).* [http://dx.doi.org/10.1063/1.4954650]

Distributed feedback (DFB) lasers are one of the most versatile and efficient laser structures. Examples include DFB semiconductor lasers for telecommunications,[1] polymer based organic lasers for explosive sensing,[2] nanoimprinted vitamin,[3] and DNA[4] lasers for bio applications and single mode optofluidic DFB lasers.[5–7] Especially, optofluidic DFB lasers have attracted substantial attention due to their potential for cost-effective lab-on-a-chip spectroscopy applications.[8,9] Compared with whispering gallery mode resonators and Fabry–Pérot like cavities, the DFB structure is particularly well suited for achieving narrow bandwidth single-mode lasing operation. Single-mode operation is often desirable, e.g., for high resolution spectroscopy and sensing, in part because it simplifies the monitoring of changes in the emission spectrum. Moreover, the periodic structure of DFB gratings gives rise to a well-defined photonic band structure which allows the measurement of optical parameters even below threshold.[10,11]

The most common design for optofluidic DFB lasers is based on a gain doped liquid core waveguide structure as this configuration readily satisfies the need for a substantial overlap of the optical mode with the gain region.[12] However, such devices require the use of buffers or solvents with high refractive index, such as ethylene glycol or dimethyl sulfoxide (DMSO).[5–7,13,14] High refractive index solvents are usually not biocompatible, which limits the application of optofluidic DFB lasers in biosensing.[15]

The study of stimulated emission from biological materials has also gained substantial interest over the last two decades, from random lasing in dye stained animal tissue[16] to the development of single cell biological lasers.[17] However, in order to realize optofluidic DFB lasers with biocompatible water based gain fluids, an evanescent pumping scheme is required due to the relatively low refractive index of water. In this configuration, which was first proposed by Ippen and Shank in 1972,[18] a

polymer based waveguide core is adjacent to the gain doped fluid layer. Although the stimulated emission rate is limited due to the reduced overlap of the laser-active optical mode with the gain layer, evanescent pumped DFB lasers have been demonstrated by Song *et al.* in 2009.[19] Despite this initial success, lasing thresholds have so far remained large compared with fluid-core DFB lasers, and DMSO had to be added to the dye solution in order to enhance the mode overlap, which has prevented more widespread application of this configuration.

In this work, we fabricated and investigated an aqueous-solution-based evanescently pumped optofluidic DFB laser. As illustrated in Fig. 1, the laser comprises a substrate as bottom cladding, a polymer film, into which a grating structure is imprinted, as waveguide core, and a water-based fluorescent dye solution as upper cladding layer. By utilizing a mixed order grating and a low index substrate, we were able to demonstrate low lasing threshold of $E_{TH} = 520$ nJ which represents nearly a 20-fold reduction over the previously reported values (earlier thresholds were $E_{TH} = 9.5$ μJ; Ref. 19). The photonic angular dispersion was measured using single shot Fourier imaging to relate the spectral and spatial
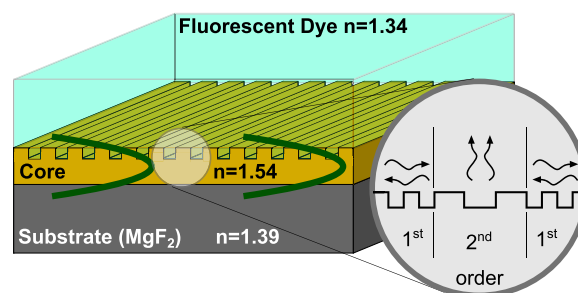

FIG. 1. Illustration of an optofluidic DFB laser. The waveguide stack consists of a substrate, a core-grating, and a gain material layer. The core layer has a thickness of several 100 nm and the substrate and gain layer have a thickness of ∼1 mm. The refractive index of the core-grating layer is greater than the refractive indices of the adjacent layers. On the mixed-order grating, the 1st order is used for in plane feedback and the 2nd order for outcoupling perpendicular to the surface.

a)Email: mcg6@st-andrews.ac.uk

108, 261101-1

emission properties below and above lasing threshold to pho-
tonic modes. This enables measurements of the waveguide
properties, such as the refractive index of the gain fluid, even
below the lasing threshold.

   To model our DFB laser structure, it was decomposed
into an asymmetric waveguide and a grating structure. We
chose a two-dimensional simulation approach because our
structure is planar. For the DFB laser to operate efficiently,
the waveguide needs to support and confine the optical
modes. For a dielectric three layer slab waveguide, the opti-
cal modes fulfill the relation[20]

$$\frac{4\pi d}{\lambda_0}\sqrt{n_g^2 - n_{eff}^2} = \phi_a + \phi_s + 2M\pi, \tag{1}$$

where d is the thickness of the waveguide core, λ_0 is the vac-
uum wavelength, n_g the refractive index of the waveguide
layer, n_{eff} the effective refractive index of the mode, $\phi_{a/s}$ the
Goos–Hänchen phase shift at the interface between wave-
guide layer and each cladding layer, and M is an integer.

   Light is Bragg scattered by the corrugation at the inter-
face between the solid waveguide core and the liquid gain
cladding layer. The scattering angle depends on the wave-
length of the propagating mode and can be described by[21]

$$\frac{2\pi}{\lambda}\sin\theta = \pm\frac{2\pi n_{eff}}{\lambda} \pm m\frac{2\pi}{\Lambda}, \tag{2}$$

where λ is the wavelength, θ is the free-space scattering
angle, Λ is the grating period, and m is an integer.
Distributed feedback occurs when the grating diffracts the
mode into the counter propagating mode, i.e., if the Bragg
condition $m\lambda = 2n_{eff}\Lambda$ is satisfied.

   Using Eq. (1) and solving the Helmholtz equation with
appropriate boundary conditions, we determined the electric
field distribution within the three layer dielectric waveguide.
Fig. 2(a) shows the case for the TE0 mode. For an SiO$_2$ sub-
strate (dashed line, $n_{SiO_2} = 1.46$) the mode is highly asymmet-
ric, with a significant fraction of the mode located in the
substrate. Therefore, the overlap factor Γ of the mode with the
gain medium is only 11.7 % (assuming a core layer thickness
of $d = 300$ nm). Changing the substrate material to MgF$_2$
($n_{MgF_2} = 1.39$) renders the TE0 mode more symmetric, lead-
ing to an increased overlap with the gain layer ($\Gamma = 18.4$ %).
This is due to the lower refractive index of MgF$_2$ compared
with SiO$_2$.

   The waveguide core thickness also influences the confine-
ment of the mode and hence the overlap with the gain layer
(Fig. 2(b)). For the MgF$_2$ substrate the mode overlap contin-
ues to increase with decreasing core thickness across the entire
range modeled here. However, for the SiO$_2$ substrate it satu-
rates for core layer thicknesses <300 nm with a cut-off thick-
ness of $d_{cut} = 168$ nm. For all core layer thicknesses, the
overlap for MgF$_2$ substrate exceeds the overlap for SiO$_2$-based
devices. On an MgF$_2$ substrate, waveguide modes are no lon-
ger supported if the core layer thickness is reduced below
66 nm (not shown in Fig. 2(b)). For a layer thickness above
450 nm (MgF$_2$ substrate) and 700 nm (SiO$_2$ substrate), respec-
tively, TE1 and TM1 modes are supported by the waveguide
structure. Exceeding these thicknesses is not desirable as it
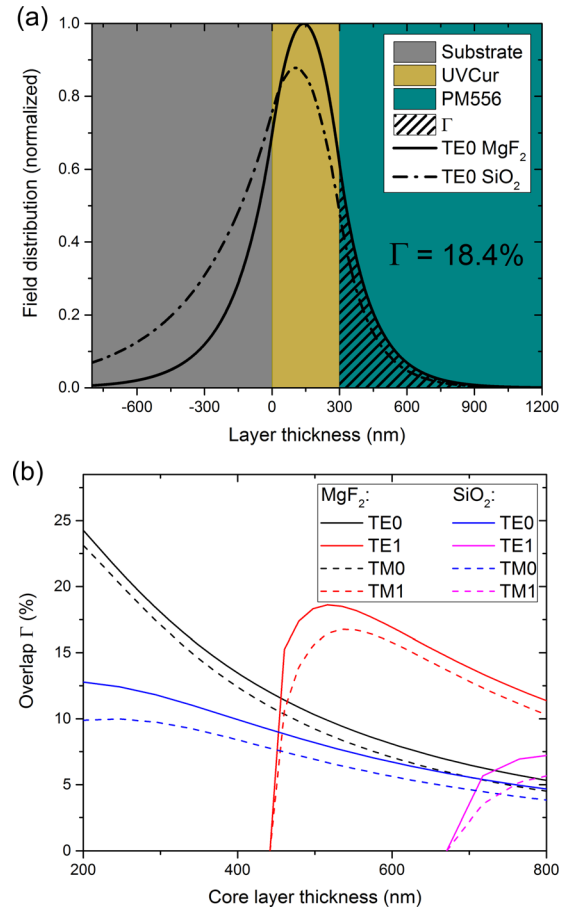could lead to mode beating and multi-mode lasing.

FIG. 2. (a) TE0 mode simulation for the waveguide stack formed by substrate,
core-grating (UV-Cur06) and gain material (PM556). The dashed line shows
the TE0 mode for a SiO$_2$ substrate for a core layer thickness of $d = 300$ nm.
The overlap with the gain layer for this case is $\Gamma = 11.7\%$. The solid line shows
the TE0 mode for an MgF$_2$ substrate. The mode is more symmetrical and an
enhanced overlap with the gain layer of $\Gamma = 18.4\%$ is seen. (b) Simulated
mode overlap with the gain layer for different core layer thicknesses, substrate
materials, and polarizations (TE and TM). The highest overlap is achieved with
MgF$_2$ substrates and a core layer thickness of $d < 300$ nm.

   The DFB lasers fabricated here consist of a 25 mm $\times$ 25 mm
MgF$_2$ or SiO$_2$ substrate, a UV-curable crosslinked polymer
film as waveguide core (mr-UVCur06, Microresist
Technologies , $n = 1.54$), and a dye doped water droplet as
gain layer ($n = 1.34$). All stated refractive indices are for a
wavelength $\lambda = 530$ nm. The mr-UVCur06 layer was spin
coated onto the substrate, and by varying the spinning parame-
ters, different layer thicknesses ranging from 250 nm to
600 nm were achieved. We used a UV-nanoimprint lithogra-
phy process as described in detail by Wang *et al.*[22] to pattern
the grating onto the mr-UVCur06 layer. A detailed characteri-
zation of this grating and corresponding SEM images can be
found in Ref. 22.

   To achieve low threshold lasing, a one dimensional
mixed-order grating was used. Utilizing such a mixed-order
grating, very low lasing thresholds down to 57 W/cm^2 were
previously achieved for organic semiconductor based DFB
lasers.[22] The grating used here consisted of two first-order
regions, with 2860 grating periods of $\Lambda = 175$ nm, separated
by a central second-order region, which had a grating period
of $\Lambda = 350$ nm and between 4 and 12 repetitions. The total
area of each grating was 1 mm $\times$ 1 mm. Due to Bragg

scattering, the first-order region supports in-plane optical feedback and the smaller second-order region provides surface outcoupling by scattering the mode out of plane perpendicular to the surface via first-order diffraction (see inset in Fig. 1).[2]

The gain layer consisted of an aqueous solution of the fluorescent dye Pyrromethene 556 (PM556, Disodium-1,3,5,7,8-pentamethylpyrromethene-2,6-disulfonate-difluoro-borate, Exciton, Inc.). Concentrations of 0.8 to 5 mmol/l of PM556 were dissolved in deionized water and a droplet of the solution (10 μl) was then placed on the grating structure. The amount of dye solution was sufficient to avoid evaporation for more than 10 min of continuous pumping. In addition, photobleaching was avoided due to convection inside the droplet, which replenished the fluorophores in the volume close to the feedback structure.

In order to investigate the photonic band structure of our DFB structures, the DFB gratings were illuminated with a broad band halogen lamp through a microscope objective. The reflectance of the grating was collected with the same objective and the Fourier plane of the objective was imaged onto the entrance slit of a spectrometer in order to resolve the angle dependence of the reflectivity.[23] The structure transmits most of the incident light, but a fraction of the light is coupled to the waveguide and scattered back at the angles at which Eq. (2) is satisfied. In this way we were able to measure the angle dependent photonic dispersion over a range of $\pm 33°$ using a $40\times$ ($NA = 0.55$) objective. A measurement of the photonic band structure of a SiO_2-based second-order DFB grating region with $\Lambda = 350$ nm and with air as the top layer is shown in Fig. 3(a). Fitting Eq. (2) to the photonic bands and solving Eq. (1) yields a core layer thickness of $d = (554 \pm 7)$nm, which is still below the onset thickness for TE1 and TM1 modes in SiO_2-based devices (Fig. 2(b)). As can be seen in the inset of Fig. 3(a), a characteristic photonic stop band opens at 0° angle and the resonance wavelength $\lambda_{res} = (527.7 \pm 0.2)$nm.

Next, the fluorescent dye solution was excited by direct pumping through the substrate and the grating (similar pump configuration as used by Song *et al.*[19]) using a pulsed optical parametric oscillator (OPO) system tuned to 480 nm (20 Hz repetition rate and 5 ns pulse length, pump energy <100 nJ). In this configuration, dye molecules in a volume above the waveguide are excited. Fig. 3(b) shows the angle-resolved photoluminescence of the grating discussed before, but now with a droplet of aqueous PM556 solution as the top layer. The data indicate that a portion of the fluorescence generated by the dye is coupled to the waveguide and then scattered to the top and bottom by the DFB grating. This led to a reduction in the recorded fluorescence signal along the photonic bands. Fitting Eq. (2) to the photonic bands and solving Eq. (1) yields a refractive index of the dye solution of $n = 1.342 \pm 0.015$.

In order to test lasing in the MgF_2-based structures, we increased the pump energy from the OPO. Using the same pump scheme, the image plane of the objective was now imaged onto the entrance slit of the spectrometer. The pump spot was aligned on the grating, for maximum emission intensity. Emission spectra for a range of pump energies are shown in Fig. 4(a). Below $E = 338$ nJ we observe a broad
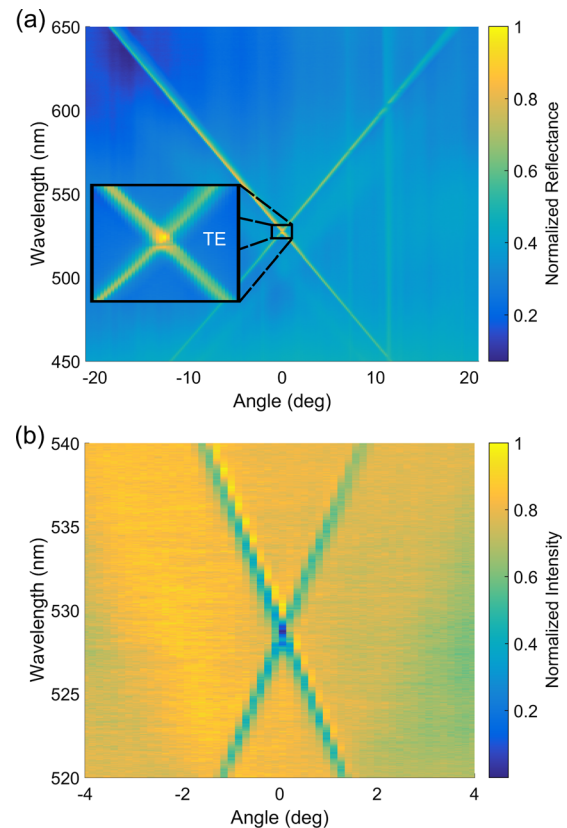

FIG. 3. Angular dispersion measurement. (a) Reflectance measurement of a SiO_2-based second-order DFB grating region with air as the top layer. Most of the light is transmitted and only a fraction is coupled to the waveguide and Bragg scattered back. The angular dispersion allows determining the core layer thickness. (Inset: Zoom-in of the region around the resonance wavelength). (b) Fluorescence measurement of the DFB grating with a dye droplet on top. A portion of the emitted fluorescence is coupled to the waveguide and scattered in both directions by the DFB grating. This leads to a reduced signal along the photonic band structure. The pump power during the measurement shown here was well below the lasing threshold.

emission spectrum, attributed to background fluorescence from the dye. At $E = 667$ nJ, a weak peak starts to appear and then quickly gains in absolute and relative intensity as the pump pulse energy is increased further. The width of this peak is below the resolution limit of the spectrometer ($\Delta\lambda < 0.07$ nm). We attribute the peak to single mode laser operation of our DFB laser structure and argue that the optimized core thickness prevents higher order modes from propagating in the waveguide. Fig. 4(b) shows the input–output characteristics of the optofluidic DFB laser. A clear threshold is observed at $E_{TH} = 520$ nJ. This value is nearly 20-fold lower than previous reports on evanescently pumped DFB lasers[19] and within the same order of magnitude as conventional, non-evanescently pumped liquid core waveguide lasers (90 − 157 nJ).[13] We attribute the reduction in threshold over previous evanescently pumped structures to the low index substrate material, the mixed-order grating, and the optimized core layer thickness ($d = 250$ nm). A further reduction in thickness would potentially reduce the threshold even more (compare Fig. 2(b)). However, the UV curable resist used in this work did not allow fabricating thinner layers.

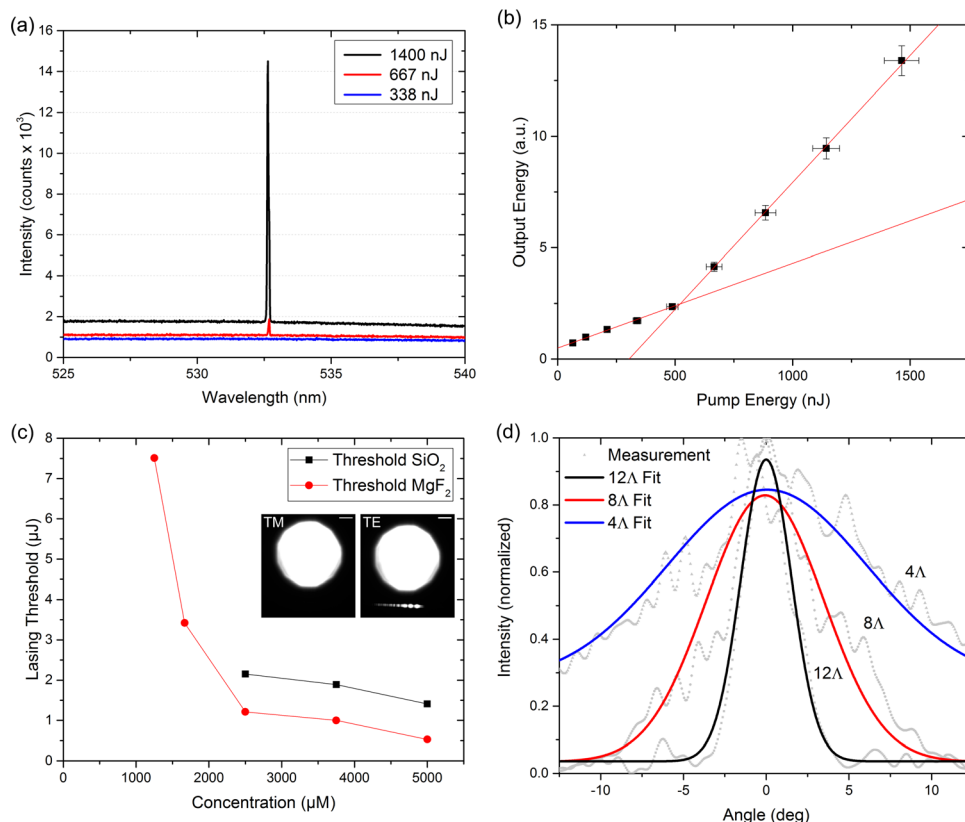Fig. 4(c) shows that the threshold pump energy for lasing depends on the dye concentration as well as the substrate

FIG. 4. (a) Emission spectra of the DFB dye laser (MgF$_2$ substrate; core thickness, 250 nm) using a dye concentration of 5 mM. The spectra are shown for a pump energy well below, at, and well above, the lasing threshold. Above threshold a distinct lasing peak is visible. (b) Input–output characteristics of the same DFB dye laser. The output energy increases nonlinearly with the pump energy and the lasing threshold is $E = 520$ nJ. (c) Change of the lasing threshold with dye concentration and substrate material. The inset shows a real image of the excitation area (round spot, positioned on the 1st order grating) and the region of laser emission (line-shaped area corresponding to the 2nd order area) for TE and TM polarization (scale bars, 50 μm). (d) Angular spread of the DFB laser emission depending on the number of 2nd order periods (4, 8, or 12 periods Λ, gray lines). The colored lines represent Gaussian fits to the data.

material. For high dye concentrations ($c = 2.5$ mM $- 5$ mM) the threshold energy decreases as the concentration increases, due to the higher chromophore density providing higher gain. For dye concentrations lower than 2.5 mM, there is a sudden dramatic increase in threshold energy, as cavity losses now dominate and the remaining chromophore density is not sufficient to compensate the losses.[24] In addition, the lasing threshold for MgF$_2$-based devices is smaller than the threshold for SiO$_2$-based devices which confirms the benefit of improved overlap between the laser active mode and the gain layer (see also Fig. 2(a)).

The inset in Fig. 4(c) shows a top view image of the mixed-order grating during lasing operation for TM and TE polarized emission. The circular bright area (Ø $= 250$ μm) is the pump spot, which is located on the first-order grating region, and the line-shaped element is the laser emission from the second-order grating region. The laser emission is highly polarized, with lasing primarily present for TE modes. We attribute this to the higher overlap for TE modes in the waveguide with the gain region (see also Fig. 2(b)). In addition, it is clear that emission and excitation are spatially separated which is due to the design of the mixed-order grating. While optical gain and feedback occur only in the area of the pump spot, the waveguide allows modes to propagate to the second-order region where the amplified lasing mode is Bragg-scattered perpendicular to the surface.

We also analyzed the angle-resolved emission of our optofluidic DFB structures above lasing threshold. According to coupled wave theory and Eq. (2), the laser light extracted by the second-order grating should be perpendicular to the surface. However, in practice, divergence arises due to the finite size of the emission source. Figure 4(d) shows the angular spread of the emission for a series of DFB lasers with a different number of second-order periods (4, 8, and 12 periods). The emission diverges with a half width of $\Delta\theta = (3.41 \pm 0.32)^\circ$ for a DFB laser with 12 periods of second-order grating. With a decreasing number of second-order periods, the divergence of the laser emission increases, i.e., by decreasing the waist of the laser beam at the source, its angular spread increases. Hence, the divergence of a surface emitted laser beam can be tailored for different applications by adjusting the number of second-order periods to couple out the light.

In conclusion, we have presented an evanescently pumped water-based single-mode optofluidic DFB laser with a record low pump threshold of $E_{TH} = 520$ nJ. The experiment shows that the threshold of the device can be considerably decreased by choosing a low index substrate material, a mixed-order grating design, and a highly concentrated dye solution. This reduction in threshold might pave the way for applications of water based optofluidic DFB lasers in areas where evanescent pumping is required, e.g., in biosensing. Our passive and active photonic dispersion analysis enables

a precise measurement of device and grating parameters. Furthermore, the divergence of the laser emission can be tailored by the number of second-order periods used for extracting the light.

[1]H. Ghafouri-Shiraz, *Distributed Feedback Laser Diodes and Optical Tunable Filters* (John Wiley & Sons, 2004).

[2]I. D. W. Samuel and G. A. Turnbull, Chem. Rev. **107**, 1272 (2007).

[3]C. Vannahme, F. Maier-Flaig, U. Lemmer, and A. Kristensen, Lab Chip **13**, 2675 (2013).

[4]A. Camposeo, P. Del Carro, L. Persano, K. Cyprych, A. Szukalski, L. Sznitko, J. Mysliwiec, and D. Pisignano, ACS Nano **8**, 10893 (2014).

[5]Z. Li, Z. Zhang, T. Emery, A. Scherer, and D. Psaltis, Opt. Express **14**, 696 (2006).

[6]M. Gersborg-Hansen and A. Kristensen, Opt. Express **15**, 137 (2007).

[7]A. Bakal, C. Vannahme, A. Kristensen, and U. Levy, Appl. Phys. Lett. **107**, 211105 (2015).

[8]T. Wienhold, F. Breithaupt, C. Vannahme, M. Brøkner Christiansen, W. Dörfler, A. Kristensen, and T. Mappes, Lab Chip **12**, 3734 (2012).

[9]L. Pang, H. M. Chen, L. M. Freeman, and Y. Fainman, Lab Chip **12**, 3543 (2012).

[10]G. A. Turnbull, P. Andrew, M. J. Jory, W. L. Barnes, and I. D. W. Samuel, Phys. Rev. B **64**, 125122 (2001).

[11]P. Andrew, G. A. Turnbull, I. D. W. Samuel, and W. L. Barnes, Appl. Phys. Lett. **81**, 954 (2002).

[12]Y. Fainman, L. Lee, D. Psaltis, and C. Yang, *Optofluidics: Fundamentals, Devices, and Applications*, 1st ed. (McGraw-Hill, Inc., New York, NY, USA, 2010).

[13]W. Song, A. E. Vasdekis, Z. Li, and D. Psaltis, Appl. Phys. Lett. **94**, 051117 (2009).

[14]Z. Li, Z. Zhang, A. Scherer, and D. Psaltis, in *Proceedings of the 2008 Digest of the IEEE/LEOS Summer Topical Meetings* (2006), Vol. 14, p. 58.

[15]X. Fan and S.-H. Yun, Nat. Methods **11**, 141 (2014).

[16]M. Siddique, L. Yang, Q. Z. Wang, and R. R. Alfano, Opt. Commun. **117**, 475 (1995).

[17]M. C. Gather and S. H. Yun, Nat. Photonics **5**, 406 (2011).

[18]E. P. Ippen and C. V. Shank, Appl. Phys. Lett. **21**, 301 (1972).

[19]W. Song, A. E. Vasdekis, Z. Li, and D. Psaltis, Appl. Phys. Lett. **94**, 161110 (2009).

[20]A. B. Buckman, *Guided-Wave Photonics* (Saunders College Publishing, 1992).

[21]H. Kogelnik, J. Appl. Phys. **43**, 2327 (1972).

[22]Y. Wang, G. Tsiminis, A. L. Kanibolotsky, P. J. Skabara, I. D. W. Samuel, and G. A. Turnbull, Opt. Express **21**, 14362 (2013).

[23]C. P. Dietrich, S. Höfling, and M. C. Gather, Appl. Phys. Lett. **105**, 233702 (2014).

[24]J. Weber, Z. Phys. **258**, 277 (1973).